

# MicroRNA-449b-3p inhibits epithelial-mesenchymal transition by targeting IL-6 and through the JAK2/STAT3 signaling pathway in non-small cell lung cancer

KAI CAI, HONG-XIA LI, PAN-PAN LI, ZI-JIAN GUO and YANG YANG

Department of Oncology, The First Affiliated Hospital of Guangxi University of  
Traditional Chinese Medicine, Nanning, Guangxi 530000, P.R. China

Received August 31, 2019; Accepted January 10, 2020

DOI: 10.3892/etm.2020.8504

**Abstract.** MicroRNAs (miRs) have vital involvement in the advancement of non-small cell lung cancer (NSCLC); however, the methods of action of miR-449b-3p in the disease are yet to be examined. The present study revealed a distinct downregulation of miR-449b-3p in NSCLC tissue, which was related to the clinicopathological characteristics, and may serve as an independent marker for NSCLC prognosis. NSCLC cell epithelial-mesenchymal transition (EMT), metastasis and migration were distinctly controlled *in vitro* by miR-449b-3p, that was found to directly target interleukin (IL)-6. Additionally, increased IL-6 level could inhibit miR-449b-3p and suppress the effect of EMT in NSCLC cells by inactivating the Janus kinase 2 (JAK2)/STAT3 signaling pathway. In conclusion, the data from the present study demonstrated that IL-6 is targeted by miR-449b-3p, which affects the JAK2/STAT3 signaling pathway, impacting on the development of NSCLC.

## Introduction

Lung cancer is one of the most rapidly growing types of cancer that is associated with a high rate of morbidity worldwide (1,2). Non-small cell lung cancer (NSCLC) constitutes ~80% of lung cancer cases, inclusive of adenocarcinomas as well as squamous cell carcinomas (1). The prognosis is poor owing to inefficient therapeutic approaches during the early and advanced stages of the disease, as well as the frequency of relapses, making the 5-year survival rate <15% (3). As

such, it is necessary to investigate the mechanisms of action behind the pathogenesis of NSCLC to identify new therapeutic approaches.

MicroRNAs (miRNAs/miRs) are a set of small, non-coding RNAs that are 20-24 nucleotides in length and are highly evolutionarily conserved (4). miRNAs bind to the 3'-untranslated regions (UTRs) of target mRNAs to either degrade the target, or prevent further expression (5). Alterations in miRNA expression levels are linked to the initiation and development of several types of cancer (6-10). While the involvement of many miRNAs has been reported in the development of NSCLC (11,12), the use of these molecules for therapy is limited (13), with their exact functions and mechanisms of action in tumorigenesis remaining unclear. For example, miR-449 shows atypical levels in many cancer types with variations between different tumors. miR-449 plays an important role in gynecological clear cell carcinoma (14), hepatocellular cancer (15), papillary thyroid carcinoma (16) and breast cancer (17). Despite this evidence, the mechanism of action in NSCLC remains to be established.

The current study reported decreased levels of miR-449b-3p in NSCLC tumor tissues compared to adjacent normal tissues, with a negative association with tumor stage and metastasis to lymph nodes. miR-449b-3p overexpression caused the inhibition of migration, metastasis and NSCLC cell epithelial-mesenchymal transition (EMT) *in vitro*. Additionally, the targeting of interleukin (IL)-6 mRNA, as well as downregulation of the Janus kinase 2 (JAK2)/STAT3 pathway by miR-449b-3p, was shown in the cell lines. This work highlighted the ability of miR-449b-3p to suppress NSCLC and identified one of its molecular targets as IL-6.

## Materials and methods

**Patients and tissue details.** NSCLC tumor tissue and neighboring adjacent normal tissue (61 pairs) were collected from surgical lung resection samples, subject to patients presenting clinicopathological characteristics of NSCLC, with no prior radiotherapy or chemotherapy. Samples were collected from the lesion edges, which were confirmed by a minimum of two experienced pathologists, at The First Affiliated Hospital of Guangxi University of Traditional Chinese Medicine between

---

**Correspondence to:** Dr Yang Yang, Department of Oncology, The First Affiliated Hospital of Guangxi University of Traditional Chinese Medicine, 6 Shuangyong Road, Nanning, Guangxi 530000, P.R. China  
E-mail: 2574469708@qq.com

**Key words:** microRNA-449b-3p, epithelial-mesenchymal transition, non-small cell lung cancer, interleukin-6, Janus kinase 2/STAT3 pathway

January 2011 and December 2013. Liquid nitrogen was used to freeze the samples, followed by  $-80^{\circ}\text{C}$  storage for the analysis. The ethics committee of the First Affiliated Hospital of Guangxi University of Traditional Chinese Medicine (Nanning, China) issued approval of the collection of patient samples. The ethics approval number is GKG-1407014.

**Cell culture and transfection.** The NSCLC cell lines A549, H1299, CALU-1, H520 and H1703, in addition to the 293T and Beas-2b normal human bronchial epithelial cell lines, were supplied by The Cell Bank of Type Culture Collection of the Chinese Academy of Sciences. RPMI-1640 (Gibco; Thermo Fisher Scientific, Inc.) supplemented with 10% FBS (Gibco; Thermo Fisher Scientific, Inc.), 100  $\mu\text{g}/\text{ml}$  streptomycin and 100 U/ml penicillin (Gibco; Thermo Fisher Scientific, Inc.) was used for cell-culture. Unless otherwise stated, cells were incubated at  $37^{\circ}\text{C}$  and 5%  $\text{CO}_2$  in a humidified atmosphere. miR-449b-3p mimics, miR-449b-3p inhibitors and the corresponding miR-control (scrambled/non-coding control) were purchased from Sigma-Aldrich; Merck KGaA. The sequences were as follows: miR-449b-3p mimic, 5'-CAGCCACAACUACCCUGCCACU-3'; miR-449b-3p mimic control, 5'-UUCUCCGAACGUGUCACGUTT-3'; miR-449b-3p inhibitor, 5'-ACAAAGGACAGUCUGCUCCUG-3'; and miR-449b-3p inhibitor control, 5'-CAGUACUUUUGUGUAGUACAA-3'.

To study the roles of miR-449b-3p in the progression of NSCLC *in vitro*, A549 and H1299 cells ( $2 \times 10^3$  cells/ml) were seeded into a 96-well plates and transfected using Lipofectamine<sup>®</sup> 2000 (Thermo Fisher Scientific, Inc.) with the miR-449b-3p mimic (50 nM), miR-449b-3p inhibitor (50 nM) or corresponding controls (50 nM) for 48 h, according to manufacturer's protocols. In addition, an overexpression vector encoding IL-6 (termed IL-6; Shanghai GenePharma Co., Ltd.) and corresponding control vector (termed pcDNA-NC; Shanghai GenePharma Co., Ltd.) was transfected into A549 cells according to manufacturer's protocol. A co-transfection group was also created for A549 cells, which were co-transfected with IL-6 (100 nM) and miR-449b-3p mimic (50 nM; termed IL-6 + miR-449b-3p mimic). Subsequent experimentation was performed at 48 h after transfection.

**Reverse transcription-quantitative PCR (RT-qPCR).** TRIzol<sup>®</sup> reagent from Invitrogen; Thermo Fisher Scientific, Inc. was employed for isolating total RNA from samples, in accordance with the manufacturer's protocols. Total RNA was converted into first-strand cDNA using a Mir-X<sup>™</sup> miRNA First-Strand Synthesis kit (Takara Bio, Inc.) for miRNAs or PrimeScript<sup>™</sup> RT Reagent kit (Takara Bio, Inc.) for mRNAs per the prescribed protocols of the manufacturer. The temperature conditions for reverse transcription were as follows:  $37^{\circ}\text{C}$  for 15 min followed by  $85^{\circ}\text{C}$  for 5 sec. Subsequent qPCR was performed using SYBR<sup>®</sup> Premix Ex Taq II (Takara Bio, Inc.) and a ViiA 7 real-time PCR system from Applied Biosystems; Thermo Fisher Scientific, Inc. in accordance with the prescribed protocols of the manufacturer. The levels of miR-449b-3p were normalized to U6, whereas the levels of IL-6 were normalized to that of  $\beta$ -actin and quantified using the  $2^{-\Delta\Delta\text{Ct}}$  method (18). U6 or  $\beta$ -actin was measured as an internal control. The thermocycling conditions were as follows: Initial denaturation

at  $95^{\circ}\text{C}$  for 10 min, followed by 40 cycles of  $95^{\circ}\text{C}$  for 20 sec and  $60^{\circ}\text{C}$  for 45 sec. The RT-qPCR primers were as follows: miR-449b-3p forward, 5'-CCTGGACGGCACGAAA-3' and reverse, from the aforementioned kit; U6 forward, 5'-CTCGCTTCGGCAGCACA-3' and reverse, 5'-AACGCTTCACGAATTGCGT-3'; IL-6 forward, 5'-CCTAATTAGGCATCGGAA-3' and reverse, 5'-ACGACACAGCGAACACAACGTC-3'; and  $\beta$ -actin forward, 5'-TGACGTGGACATCCGCAAAG-3' and reverse, 5'-CTGGAAGGTGGACAGCGAGG-3'.

**In vitro cell assays for migration and invasion.** The ability of cells to migrate and invade was assessed using Transwell assays and wound healing assays. The Transwell migration assay involved placing  $2 \times 10^4$  cells in RPMI-1640 (Gibco; Thermo Fisher Scientific, Inc.) medium without serum into the upper chamber of a well with an 8- $\mu\text{m}$  pore insert (Corning, Inc.). The Transwell invasion assay involved seeding  $4 \times 10^4$  cells in medium without serum into the upper chamber, precoated with Matrigel<sup>®</sup> (Corning, Inc.) for 48 h at  $37^{\circ}\text{C}$ . For both the Transwell migration and invasion assays, the lower chamber contained medium with 20% FBS. Following 24 h incubation at  $37^{\circ}\text{C}$ , cotton swabs were used to remove non-migrating cells. Fixation of the cells on the lower membrane that had migrated or invaded was performed using 4% paraformaldehyde for 30 min at  $25^{\circ}\text{C}$  followed by crystal violet staining for 30 min at  $25^{\circ}\text{C}$ . Invading and migrating cells were counted from 10 randomly selected fields using a light microscope (magnification,  $\times 40$ ; Olympus Corporation).

**Western blotting.** RIPA lysis buffer (Beyotime Institute of Biotechnology) containing protease inhibitor was used to extract the total proteins from samples for 20 min on ice. After the measurement of protein concentration using Bradford's reagent (Beyotime Institute of Biotechnology), Total protein (25  $\mu\text{g}$ ) was separated by 10% SDS-PAGE was run to resolve samples, followed by transfer onto PVDF membranes. Non-fat milk (5%) in TBST was used for blocking for 60 min at room temperature, followed by overnight incubation with primary antibodies at  $4^{\circ}\text{C}$ . The following antibodies were used: E-cadherin (1:1,000; cat. no. ab40772; Abcam), N-cadherin (1:1,000; cat. no. ab18203; Abcam), vimentin (1:1,000; cat. no. ab92547; Abcam),  $\beta$ -actin (1:5,000; cat. no. 4970T; Cell Signaling Technologies, Inc.), IL-6 (1:1,000; cat. no. 12912T; Cell Signaling Technology, Inc.), JAK2 (1:1,000; cat. no. 3230T; Cell Signaling Technologies, Inc.), phospho-JAK2 (1:1,000; cat. no. 3771T; Cell Signaling Technologies, Inc.), phospho-STAT3 (1:1,000; cat. no. 9145T; Cell Signaling Technologies, Inc.) and STAT3 (1:1,000; cat. no. MAB1799-SP; Proteintech Group, Inc.). The secondary antibody used was horseradish peroxidase-conjugated anti-rabbit (1:10,000; cat. no. ab205718; Abcam) or anti-mouse IgG (1:10,000; cat. no. HAF007; Proteintech Group, Inc.) for 1 h at  $25^{\circ}\text{C}$ . Protein expression was normalized to  $\beta$ -actin and were visualized using an enhanced chemiluminescence system (EMD Millipore). Relative expression was measured using Bio-Rad Image Lab software version 5.1 (Bio-Rad Laboratories, Inc.).

**Luciferase reporter assay.** A pMIR-REPORT luciferase vector (Invitrogen; Thermo Fisher Scientific, Inc.) was constructed

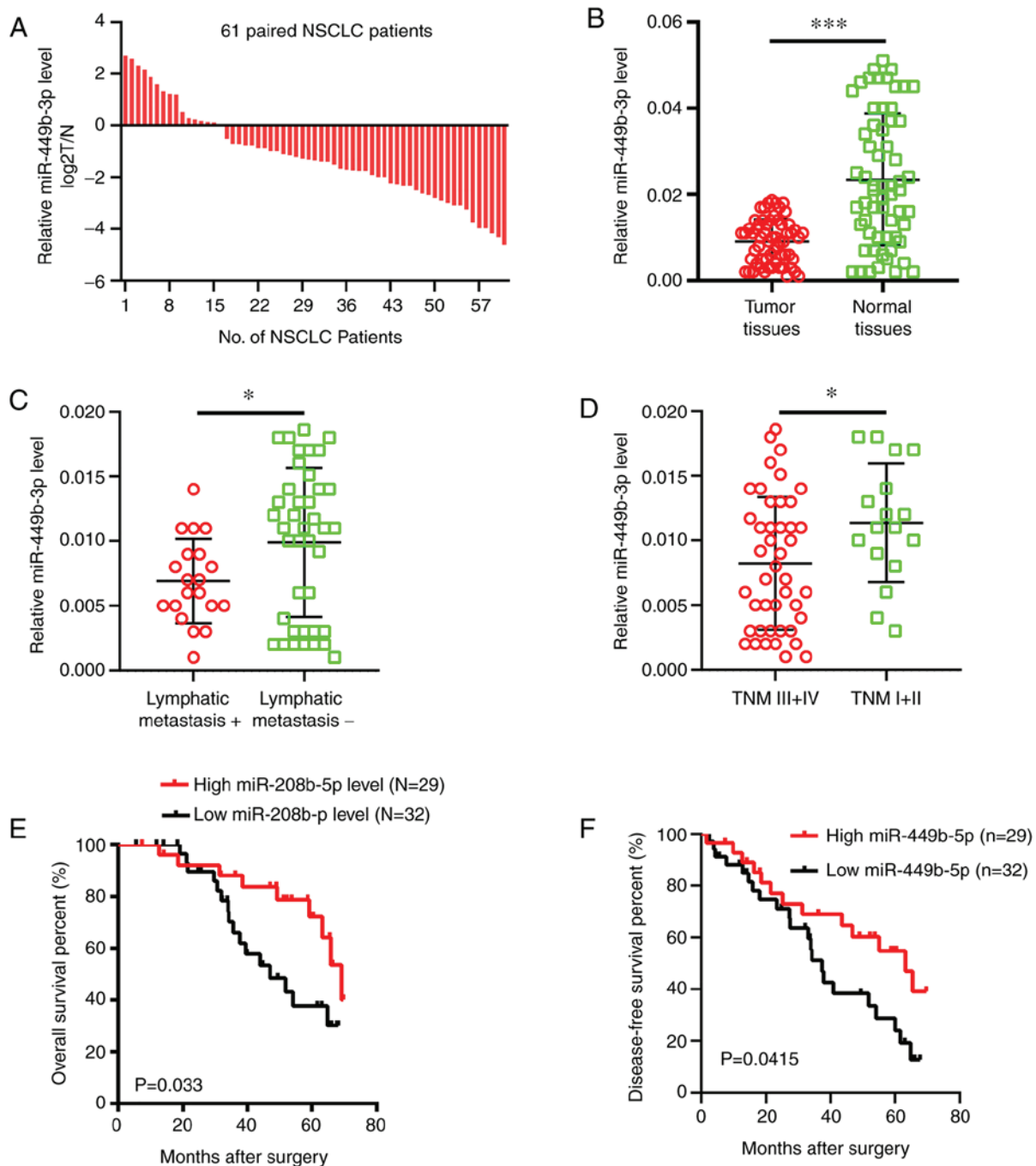


Figure 1. miR-449b-3p levels and implications in NSCLC clinical samples. (A) miR-449b-3p relative expression levels of in 61 NSCLC tumor specimens. (B) Decreased miR-449b-3p in tumor compared with neighboring healthy tissue, as shown by reverse transcription-quantitative PCR. miR-449b-3p was conspicuously lower in samples with (C) metastasis or (D) advanced TNM stage, compared with those which did not display these cancer grades. The lower levels of miR-449b-3p were associated with lower survival, both in terms of (E) overall and (F) disease-free survival, compared with increased levels of the miRNA, as shown by Kaplan-Meier analysis. \*P<0.05; \*\*\*P<0.001. miR/miRNA, microRNA; NSCLC, non-small cell lung cancer; TNM, tumor-node-metastasis.

to perform luciferase reporter assays. PCR amplification of the 3'-UTR fragments of IL-6, from the RNA samples of 293T cells, containing the potential miR-449b-3p binding sites was performed, followed by insertion into the vectors, referred to as the pMIR-IL-6-wild-type (WT) thereafter. In addition, site-directed mutagenesis of the wild type binding site was performed using a FAST site-Directed mutagenesis kit (Tiangen Biotech Co., Ltd.) to generate a vector encoding the pMIR-IL-6-mutant (MUT). 293T cells ( $1.5 \times 10^4$ ) were

seeded into 96-well plates for 24 h at 37°C followed by co-transfection with miR-449b-3p (50 nM) or negative control (50 nM) and the aforementioned constructed vectors (50 nM) using Lipofectamine® 2000 (Invitrogen; Thermo Fisher Scientific, Inc.). A Dual-Luciferase® reporter assay (Promega Corporation) was performed to assess the enzyme activity in accordance with the manufacturer's protocol. Data were normalized against the activity of the *Renilla* luciferase activity.

Table I. Association between miR-449b-3p levels and non-small cell lung cancer patient clinicopathological findings.

Variable	n	miR-449b-3p expression		P-value
		High level, n=29	Low level, n=32	
Sex				0.075
Male	51	22	29	
Female	11	8	3	
Age, years				0.553
<60	39	20	19	
>60	23	10	13	
Smoking				0.851
Yes	40	19	21	
No	22	11	11	
Pathological type				0.779
Adenocarcinoma	28	13	15	
Squamous carcinoma	34	17	17	
Tumor differentiation				0.286
Well + Moderate	49	22	27	
Poor	13	8	5	
Tumor size, cm				0.830
<3	51	25	26	
>3	11	5	6	
Lymphatic metastasis				0.014
Yes	22	6	16	
No	40	24	16	
TNM classification				0.021
I-II	22	15	7	
III-IV	40	15	25	

P-values calculated by  $\chi^2$  test. TNM, tumor-node-metastasis; miR, microRNA.

**IL-6 ELISA.** A human IL-6 ELISA kit (cat. no. ab46027; Abcam) was utilized to measure the levels of IL-6 in the normal culture medium after 48 h of culture of the various cells listed, in accordance with the manufacturer's protocol.

**Bioinformatics analysis.** The potential targets of miR-449b-3p were predicted using the Targetscan database 7.1 ([http://www.targetscan.org/vert\\_72/](http://www.targetscan.org/vert_72/)).

**Statistical analysis.** SPSS version 25.0 software (IBM Corp.) was employed for statistical analysis, and data are presented as the mean  $\pm$  SD. All experiments were repeated three times. Differences between two groups were evaluated using Student's t-test. Differences between multiple groups were evaluated using one-way ANOVA followed by Tukey's post-hoc comparisons. The association between miR-449b-3p and IL-6 was assessed using Spearman's rank correlation while patient survival curves (Kaplan-Meier) were assessed using the log-rank test. The  $\chi^2$  test was used to analyse the relationships between miR-449b-3p expression and the clinicopathological features of patients with NSCLC.  $P < 0.05$  was considered to indicate a statistically significant difference.

## Results

**Decreased miR-449b-3p in NSCLC samples and the inverse association with prognosis.** RT-qPCR was performed to analyze the miR-449b-3p levels in NSCLC samples compared with adjacent normal tissues. It was shown that there were decreased miRNA levels in tumor samples (73.8% or 45/61 samples) compared to the adjacent normal tissues (Fig. 1A), which in turn exhibited approximately double the mRNA expression levels of the tumor tissues in terms of the overall expression data (Fig. 1B). The level of miR-449b-3p was less in patients with advanced tumor-node-metastasis (TNM) stage or those with metastasis to the lymph nodes (Fig. 1C and D). Clinicopathological data were analyzed after dividing the patients into two groups according to the median miR-449b-3p expression levels. The expression levels of miR-449b-3p in the NSCLC tissue were inversely associated with the presence of lymphatic metastasis ( $P=0.014$ ) and an advanced TNM stage ( $P=0.021$ ) (Table I). Furthermore, the overall survival and disease-free survival rates were significantly reduced in patients with low levels of miR-449b-3p compared with the patients with increased levels (Fig. 1E and F). Overall, a



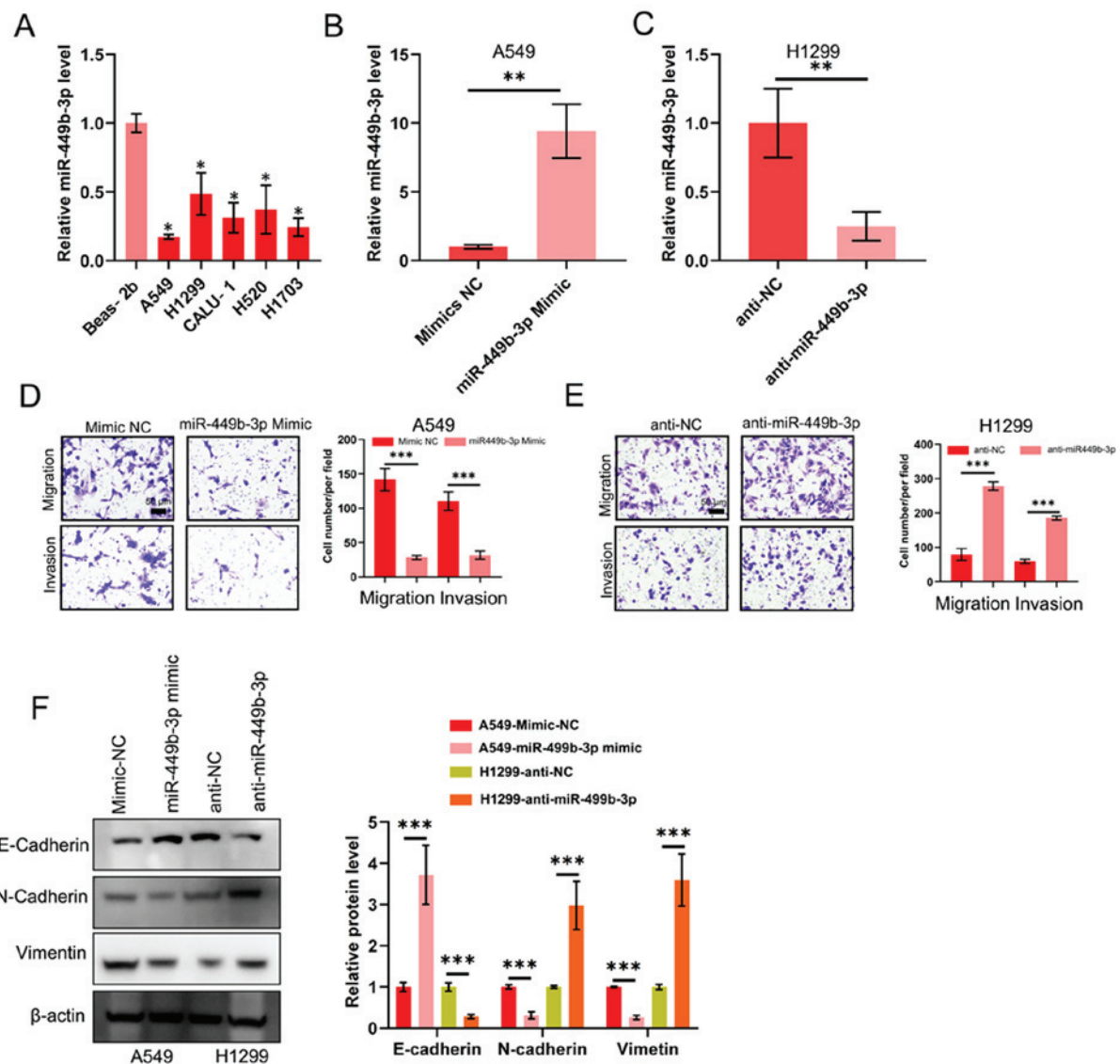


Figure 2. miR-449b-3p decreases the ability of NSCLC lines to migrate, invade and undergo epithelial-mesenchymal transition. (A) Detection of miR-449b-3p expression levels in the five NSCLC and control epithelial cell lines using reverse transcription-quantitative PCR, as analyzed using one-way ANOVA with Tukey's post-hoc comparisons. miR-449b-3p expression levels in (B) A549 and (C) H1299 cells transfected with miR-449b-3p or anti-miR-449b-3p, respectively. (D) Illustrative images and quantification of transwell assays of A549 transfected with miR-449b-3p. Scale bars, 50  $\mu$ m. (E) Illustrative images and quantification of transwell assays of H1299 transfected with anti-miR-449b-3p. Scale bars represent 50  $\mu$ m. (F) Western blot of E-cadherin, N-cadherin and vimentin in the aforementioned transfected cell lines. Right panel: Relative protein levels of E-cadherin, N-cadherin and vimentin. \*P<0.05, \*\*P<0.01 and \*\*\*P<0.001 vs. respective control. miR, microRNA; NC, negative control; NSCLC, non-small cell lung cancer.

noteworthy decline in miR-449b-3p was observed in NSCLC clinical samples, suggesting miR-449b-3p has a potential function as an independent marker of the prognosis of the disease.

**Inhibition of migration, metastasis and EMT by microRNA-331-3p.** The functions of miR-449b-3p in NSCLC metastasis was investigated on account of the association between the miRNA levels and clinicopathological data, such as metastasis. miRNA levels in the aforementioned tumor cell lines were compared against the control Beas-2b epithelial line. The tumor cell lines all displayed decreased miR-449b-3p expression compared with Beas-2b cells. Of this data, the two cell lines with the highest and lowest levels of miR-449b-3p were used for subsequent analysis: A549 and H1299 with the minimum and maximum levels, respectively (Fig. 2A). Lentivirus-based assays were performed to elevate or reduce

miR-449b-3p levels in these two lines, respectively. The effective change in expression levels were confirmed by RT-qPCR (Fig. 2B and C). Transwell assays examining the cell invasion and migration revealed a decreased number of A549 cells that could migrate and invade with raised miR-449b-3p expression levels (Fig. 2D). The opposite response was observed in H1299 cells following knockdown of miR-449b-3p. Transwell assays revealed increased cell numbers that could migrate and invade with H1299 transfected with anti-miR-449b-3p (Fig. 2E). The transfected A549 and H1299 cells were assessed for markers of EMT. Interestingly, miR-449b-3p overexpression in A549 cells significantly increased E-cadherin (a marker for epithelial tissue) expression whilst reducing those of N-cadherin and vimentin (markers of mesenchymal lineage). By contrast, the opposite trend was observed in the H1299 cells following knockdown of miR-449b-3p (Fig. 2F). In conclusion, miR-449b-3p treatment

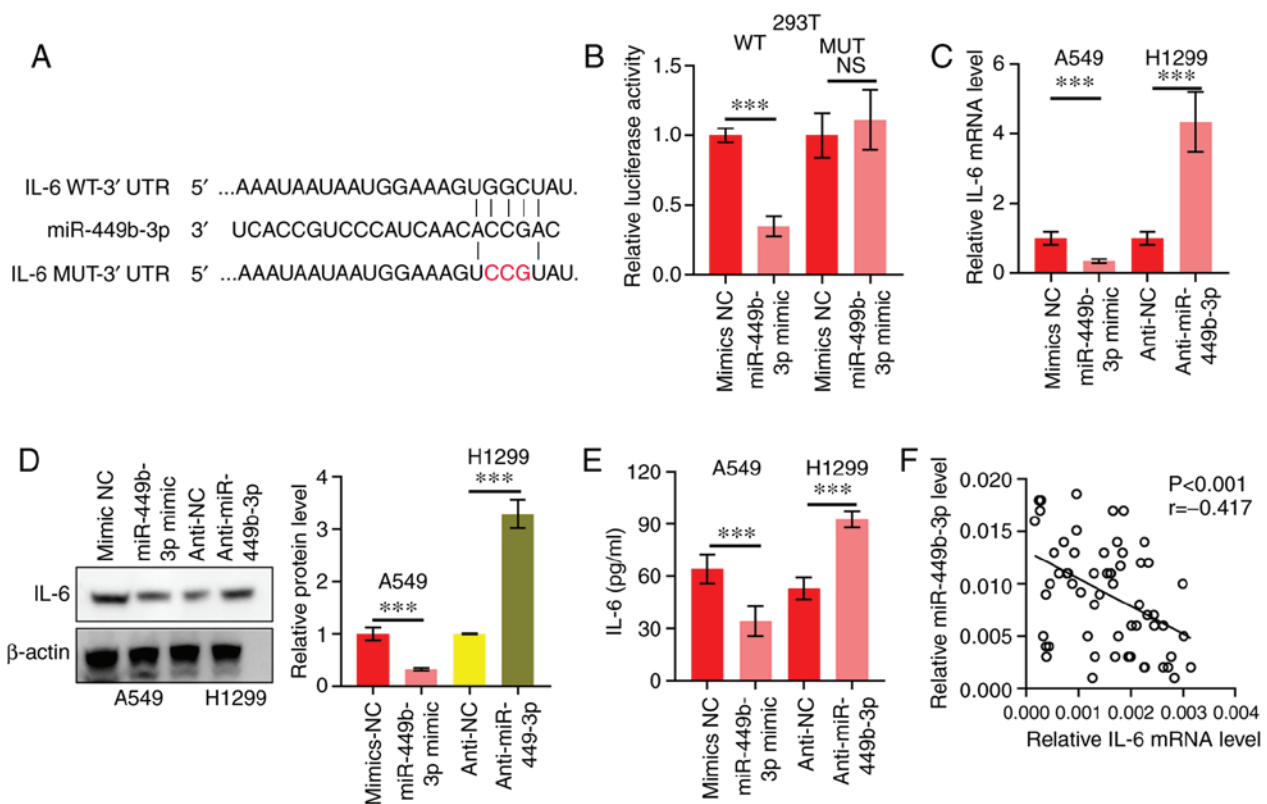


Figure 3. miR-449b-3p directly targets IL-6. (A) IL-6 WT or MUT vector construction scheme. Red letters represent bases mutated. (B) miR-449b-3p binding to IL-6, as shown by the luciferase reporter assay. Data were analyzed using Student's t-tests. (C) IL-6 mRNA of A549 and H1299 cells transfected with miR-449b-3p and anti-miR-449b-3p, respectively, assessed using reverse transcription-quantitative PCR. (D) IL-6 protein expression levels of A549 and H1299 transfected with miR-449b-3p and anti-miR-449b-3p, respectively, were assessed using western blot assays. Right panel: Relative protein expression levels of IL-6. (E) Quantification of IL-6 in the culture medium of A549 and H1299 cells transfected with miR-449b-3p and anti-miR-449b-3p, respectively. Data were analyzed using Student's t-tests. (F) Clinical specimens showing an inverse correlation between miR-449b-3p and IL-6 in NSCLC samples. Data were assessed using Spearman's rank correlation analysis. \*\*\* $P < 0.001$ . IL, interleukin; miR, microRNA; MUT, mutant; NC, negative control; NS, not significant; UTR, untranslated region; WT, wild-type.

appeared to suppress EMT of these two NSCLC lines to reduce their migratory and invasive capabilities.

**miR-449b-3p directly targets IL-6 in NSCLC.** The potential miRNA targets were predicted using the Targetscan database ([http://www.targetscan.org/vert\\_72/](http://www.targetscan.org/vert_72/)), which revealed that IL-6 was a target (Fig. 3A). This was followed by the construction and establishment of pMIR-IL-6-WT and pMIR-IL-6-MUT (Fig. 3A). 293T cells were co-transfected with miR-449b-3p and these constructs. Luciferase activity was decreased in the miR-449b-3p-transfected cells compared with those that received miR-NC. This was not observed in the pMIR-IL-6-MUT-transfected cells (Fig. 3B). Thus, the binding of miR-449b-3p to the 3'-UTR of IL-6 was confirmed. Additionally, a significant decrease in IL-6 mRNA and protein expression levels was shown by RT-qPCR and western blotting, respectively, in A549 cells (high levels of miR-449b-3p) compared with the NC. Similarly, H1299 cells with miR-449b-3p-knockdown displayed augmented levels of IL-6 mRNA and protein expression levels compared with the NC virus group (Fig. 3C and D). The ELISA also showed similar results, in that the concentration of IL-6 was significantly inhibited in the A549 cells, but significantly increased in the H1299 cells (Fig. 3E). Subsequently, RT-qPCR was used to examine the IL-6 mRNA expression levels in NSCLC tumor samples. An inverse correlation between IL-6

and miR-449b-3p was revealed ( $r = -0.417$ ,  $P < 0.001$ ; Fig. 3F). Taken together, this data indicated the direct binding of miR-449b-3p with IL-6.

**miR-449b-3p suppresses EMT through the IL-6/JAK2/STAT3 signaling pathway.** As IL-6 has been identified to be a target of miR-449b-3p in NSCLC, the mechanism of action behind the IL-6/JAK2/STAT3 network was further investigated. A549 cells were transfected with pcDNA-IL-6, which was shown to increase the mRNA expression levels of IL-6 compared to the negative control (pcDNA-NC; Fig. 4A). As shown in Fig. 4B and C, the aforementioned EMT markers and JAK2/STAT3 circuit activation were inhibited by miR-449b-3p, while this inhibitory effect on EMT and JAK2/STAT3 circuit activation was impeded by the restoration of IL-6 in the NSCLC cell lines. To summarize, the anti-cancer effects of miR-449b-3p (in terms of invasion and EMT) were shown to be mediated through JAK2/STAT3 signaling, which regulates IL-6 in NSCLC cells.

## Discussion

Research is yet to cast a complete light on the mechanisms behind NSCLC. As research has highlighted the involvement of miRNAs in the advancement and tumorigenesis of NSCLC (19), this present study explored the mechanisms of

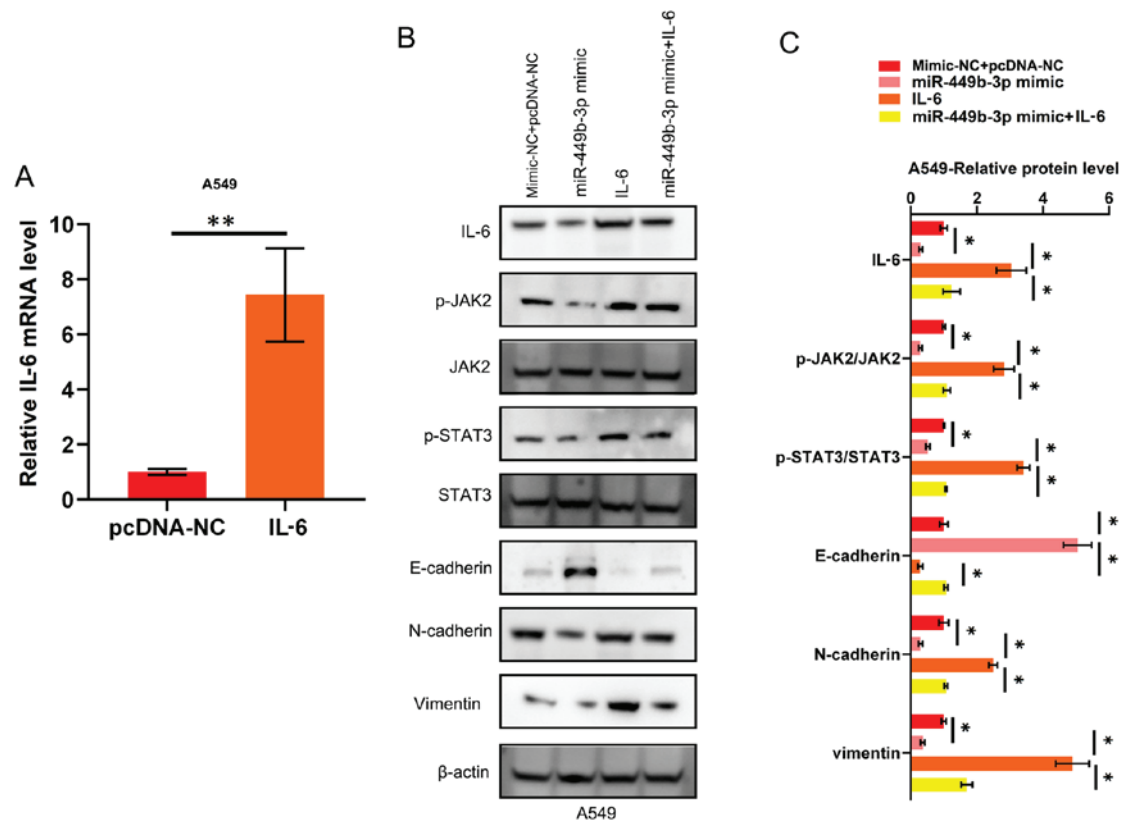


Figure 4. miR-449b-3p suppresses EMT through the IL-6/JAK2/STAT3 pathway. (A) IL-6 mRNA expression in A549 transfected with IL-6. Data were analyzed using Student's t-tests. (B) Western blotting and (C) quantification showing the activation of JAK2, and STAT3, through the phosphorylation of these proteins, as well as the suppression of EMT markers, by miR-449b-3p. This observation was reversed by IL-6 restoration. Analyzed using one-way ANOVA with Tukey's post-hoc comparisons. \* $P < 0.05$ , \*\* $P < 0.01$ . EMT, epithelial-mesenchymal transition; IL, interleukin; JAK, Janus kinase; miR, microRNA; NC, negative control.

action of miR-449b-3p in NSCLC. While previous studies have shown altered levels of miR-449b-3p in several tumors including NSCLC, the exact working in terms of targets and signaling remained to be studied (14-17). This current study corroborated the reduced miR-449b-3p levels in NSCLC samples, with its levels associated with the clinical TNM stage/metastasis as well as the overall and disease-free survival. The ability of the NSCLC cell lines studied in this present study to migrate, invade and undergo EMT was suppressed by raising the expression levels of miR-449b-3p. Furthermore, lowering the miRNA levels boosted the ability of the NSCLC cell lines to migrate and invade via EMT. This work demonstrates the cancer-inhibitory role of miR-449b-3p, as well as its role as a potential marker for the prognosis of NSCLC.

mRNAs may be targeted by miRNAs to decrease their expression. This holds true for miR-449b-3p, with research outlining several targets such as hepatocyte growth factor receptor in hepatocellular carcinoma (15), proto-oncogene RET in papillary thyroid carcinoma (16) and regulation of nuclear pre-mRNA domain containing 1B in breast cancer cells (17). In this present study, the results showed and confirmed that the cytokine IL-6 was directly targeted and regulated by the miR-449b-3p. The effects of IL-6 are pleiotropic, controlling immune and tumor functions (20). The JAK-signal transducer and STAT circuit is activated by IL-6 via the broad spectrum receptor gp130 and the specific IL-6R $\alpha$  co-receptor (21).

This is followed by dimerization and nuclear translocation of the phosphorylated STATs, leading to the expression of downstream genes of IL-6 (22). While the complete methods of action of miR-449b-3p in NSCLC are yet to be uncovered, the current results suggest that the molecule may inhibit the ability of the studied NSCLC cell lines to migrate and invade through IL-6.

The JAK/STAT pathway is an evolutionarily conserved signaling pathway that is involved in a number of basic cellular functions, such as cell growth and metastasis, which lead to the development and progression of cancer (23,24). IL-6 stimulation leads to the autophosphorylation and activation of JAK, which in turn phosphorylates STAT3. STAT3 then forms a homodimer and translocates into the cell nucleus to promote the transcription of responsive oncogenes, including c-Myc, Bcl-1, cyclin D1/D2 and Bcl-xl (25). In this present study, over-expressing miR-449b-3p was shown to inhibit the activation of the JAK2/STAT3 signaling pathway, which was rescued by overexpression of IL-6. Therefore, it was speculated that miR-449b-3p may exert a tumor suppressor role in NSCLC through the IL-6/JAK2/STAT3 pathway, which necessitates future analysis.

To summarize, downregulation of miR-449b-3p in NSCLC samples was shown in this present study, which correlated with the survival of patients and the ability of the cancer to metastasize, as well as to display EMT characteristics, through the IL-6/JAK2/STAT3 pathway.

## Acknowledgements

Not applicable.

## Funding

This study was supported by grants from the Chinese Medicine Science and Technology Special of Guangxi Autonomous Region (grant no. G2K210-096).

## Availability of data and materials

The datasets used and/or analyzed in the present study are available from the corresponding author on reasonable request.

## Authors' contributions

YY conceived the study and designed the experiments. KC and HXL provided the experimental materials. KC, HXL, and PPL performed the experiments. ZJG performed the data analysis. KC wrote the manuscript. All authors contributed to the interpretation and discussion of the results and reviewed the manuscript. All authors read and approved the final manuscript.

## Ethics approval and consent to participate

The ethics committee of the First Affiliated Hospital of Guangxi University of Traditional Chinese Medicine (Nanning, China) issued approval of the patient samples. All patients provided written informed consent.

## Patient consent for publication

Not applicable.

## Competing interests

The authors declare that they have no competing interests.

## References

1. Siegel RL, Miller KD and Jemal A: Cancer statistics, 2018. *CA Cancer J Clin* 68: 7-30, 2018.
2. Chen W, Zheng R, Baade PD, Zhang S, Zeng H, Bray F, Jemal A, Yu XQ and He J: Cancer statistics in China, 2015. *CA Cancer J Clin* 66: 115-132, 2016.
3. Heist RS and Engelman JA: SnapShot: Non-small cell lung cancer. *Cancer Cell* 21: 448.e2, 2012.
4. Bartel DP: MicroRNAs: Genomics, biogenesis, mechanism, and function. *Cell* 116: 281-297, 2004.
5. Croce CM: Causes and consequences of microRNA dysregulation in cancer. *Nat Rev Genet* 10: 704-714, 2009.
6. Wen J, Hu Y, Liu Q, Ling Y, Zhang S, Luo K, Xie X, Fu J and Yang H: miR-424 coordinates multilayered regulation of cell cycle progression to promote esophageal squamous cell carcinoma cell proliferation. *EBioMedicine* 37: 110-124, 2018.
7. Zhou YW, Zhang H, Duan CJ, Gao Y, Cheng YD, He D, Li R and Zhang CF: miR-675-5p enhances tumorigenesis and metastasis of esophageal squamous cell carcinoma by targeting REPS2. *Oncotarget* 7: 30730-30747, 2016.
8. Chang RM, Xiao S, Lei X, Yang H, Fang F and Yang LY: miRNA-487a promotes proliferation and metastasis in hepatocellular carcinoma. *Clin Cancer Res* 23: 2593-2604, 2017.
9. Song H, Li D, Wu T, Xie D, Hua K, Hu J, Deng X, Ji C, Deng Y and Fang L: MicroRNA-301b promotes cell proliferation and apoptosis resistance in triple-negative breast cancer by targeting CYLD. *BMB Rep* 51: 602-607, 2018.
10. Jiang LH, Zhang HD and Tang JH: MiR-30a: A novel biomarker and potential therapeutic target for cancer. *J Oncol* 2018: 5167829, 2018.
11. He D, Wang J, Zhang C, Shan B, Deng X, Li B, Zhou Y, Chen W, Hong J, Gao Y, *et al*: Down-regulation of miR-675-5p contributes to tumor progression and development by targeting pro-tumorigenic GPR55 in non-small cell lung cancer. *Mol Cancer* 14: 73, 2015.
12. Chen W, Wang J, Liu S, Wang S, Cheng Y, Zhou W, Duan C and Zhang C: MicroRNA-361-3p suppresses tumor cell proliferation and metastasis by directly targeting SH2B1 in NSCLC. *J Exp Clin Cancer Res* 35: 76, 2016.
13. Iqbal MA, Arora S, Prakasam G, Calin GA and Syed MA: MicroRNA in lung cancer: Role, mechanisms, pathways and therapeutic relevance. *Mol Aspects Med* 70: 3-20, 2019.
14. Jang SG, Yoo CW, Park SY, Kang S and Kim HK: Low expression of miR-449 in gynecologic clear cell carcinoma. *Int J Gynecol Cancer* 24: 1558-1563, 2014.
15. Buurman R, Gürlevik E, Schäffer V, Eilers M, Sandbothe M, Kreipe H, Wilkens L, Schlegelberger B, Kühnel F and Skawran B: Histone deacetylases activate hepatocyte growth factor signaling by repressing microRNA-449 in hepatocellular carcinoma cells. *Gastroenterology* 143: 811-820.e15, 2012.
16. Li Z, Huang X, Xu J, Su Q, Zhao J and Ma J: miR-449 over-expression inhibits papillary thyroid carcinoma cell growth by targeting RET kinase- $\beta$ -catenin signaling pathway. *Int J Oncol* 49: 1629-1637, 2016.
17. Jiang J, Yang X, He X, Ma W, Wang J, Zhou Q, Li M and Yu S: MicroRNA-449b-5p suppresses the growth and invasion of breast cancer cells via inhibiting CREPT-mediated Wnt/ $\beta$ -catenin signaling. *Chem Biol Interact* 302: 74-82, 2019.
18. Livak KJ and Schmittgen TD: Analysis of relative gene expression data using real-time quantitative PCR and the 2(-Delta Delta C(T)) method. *Methods* 25: 402-408, 2001.
19. Legras A, Pécuchet N, Imbeaud S, Pallier K, Didelot A, Roussel H, Gibault L, Fabre E, Le Pimpec-Barthes F, Laurent-Puig P and Blons H: Epithelial-to-mesenchymal transition and MicroRNAs in lung cancer. *Cancers (Basel)* 9: pii: E101, 2017.
20. Mantovani A, Allavena P, Sica A and Balkwill F: Cancer-related inflammation. *Nature* 454: 436-44, 2008.
21. Heinrich PC, Behrmann I, Haan S, Hermanns HM, Müller-Newen G and Schaper F: Principles of interleukin (IL)-6-type cytokine signalling and its regulation. *Biochem J* 374: 1-20, 2003.
22. Naugler WE and Karin M: The wolf in sheep's clothing: The role of interleukin-6 in immunity, inflammation and cancer. *Trends Mol Med* 14: 109-119, 2008.
23. Bowman T, Garcia R, Turkson J and Jove R: STATs in oncogenesis. *Oncogene* 19: 2474-2488, 2000.
24. Marotta LL, Almendro V, Marusyk A, Shipitsin M, Schemme J, Walker SR, Bloushtain-Qimron N, Kim JJ, Choudhury SA, Maruyama R, *et al*: The JAK2/STAT3 signaling pathway is required for growth of CD44(+) CD24(-) stem cell-like breast cancer cells in human tumors. *J Clin Invest* 121: 2723-2735, 2011.
25. Bromberg J and Darnell JE Jr: The role of STATs in transcriptional control and their impact on cellular function. *Oncogene* 19: 2468-2473, 2000.



This work is licensed under a Creative Commons Attribution-NonCommercial-NoDerivatives 4.0 International (CC BY-NC-ND 4.0) License.